Accurate Estimation of Posture and Velocity with Application to Coordinated Motion Control of Twin Hoisting-Girder Transporters

Zhongwei Guo[1], Yunhua Li[2]
School of Automation Science and Electrical Engineering
Beijing University of Aeronautics and Astronautics
Beijing 100083, China
1: zhongweiguo@hotmail.com, 2: yhli@buaa.edu.cn

***Abstract*—This paper proposed a novel method providing high-update rate vehicle posture and velocity estimation using Real-time Kinematics Global Position System (RTK-GPS) and simple in-vehicle speed sensors. The RTK-GPS noise processing techniques are used to discard the noises that do not satisfy the Kalman Filter model. Combining the RTK-GPS and speed sensors using extended Kalman Filter (EKF) provided a high-update rate estimation that can satisfy the need of the coordinated control of the vehicles fleet. The experimental and practical application results illustrate that the ability of the method meet the accuracy and robustness requirements of the control system.**

***Keywords*—wheeled crane, mobile robot, Kalman filter, noise processing, RTK-GPS**

I. INTRODUCTION

Reliable and accurate outdoor localization is one of the major tasks in many fields such as mapping, vehicle guidance, machine automation and mobile robots. One method in vehicle localization involves the use of relative positioning sensors, such as video cameras [1] and radar/lidar sensors [2], to determine vehicle positions relative to the road or to each other. Another option is to use the self-contained methods such as odometer and inertial navigation using inertial measurement units, however as it is well known, their accuracy decrease with time as travel distance increase due to sensor biases and integration inaccuracies [3]. The use of GPS as an external option for outdoor localization is a popular issue. Real Time Kinematics GPS (RTK-GPS), which uses C/A code and carrier phase for position calculation and uses correction signals from a base station to correct bias errors of the user receiver, can be used to provide centimeter accuracy measurement in real time. The construction machinery industry has also seen a rise in the use of GPS for precision localization and control. Although the working fields generally have a very open view of the sky and the GPS satellites, RTK-GPS alone has some characteristics, such as multi-path error, low update rate, and latency, additionally, intermittent communication loss can occur between the base station and the user receiver, which may limit its application in vehicle positioning systems.

Integration of GPS with an inertial navigation system (INS) can help to improve the positioning performance. The stability of GPS over long period of time provides the perfect complement to correct the inertial sensor drift, which results in large errors over longer period of time. Literature review shows that GPS and inertial sensors have complementary properties, and they can be fused using Kalman Filter to provide high-update rate navigation information [4]. Some research has studied the use of updating position estimates with inertial equipment between low rate (1-5Hz) GPS measurement update [5].The combination of GPS and INS has also been utilized in automotive industry to estimate vehicle's sideslip angle for automobile stability control [6].

In this paper, we proposed a kinematics estimator to provide reliable, accurate and high-update rate posture and velocity estimation for the vehicle fleet coordinated controlling. The vehicle was equipped with two RTK-GPS receivers and a few commonly used in-vehicle sensors. The incorporation of in-vehicle motion sensors is an important difference between the proposed method and a pure GPS/INS integration. This incorporation reduces the dependence of the positioning system on the high-cost INS sensors.

Although much of prior research has devoted significant effort to develop the GPS/INS-based positioning techniques in various air and land application, much of the related work is concerned solely with the navigation and dead reckoning estimation of vehicles, and not control of the vehicle. In this paper, the estimated vehicle posture and velocity are feedbacked to the fleet coordinated control system to maintain the vehicle's relative position, so the objective that dominates the design is centimeter level accuracy and fast-recovery system that provides sufficient and reliable positioning information.

The GPS signals are not always reliable, there is noise in the measurement, so we proposed a method to filter the noise before feeding them to the kinematics estimator. The remainder of this paper is organized as follows: Section II discusses the system requirements and the vehicle kinematics model; Section III describes the posture and velocities kinematics estimation

Project 50575013 supported by National Natural Science Foundation of China.

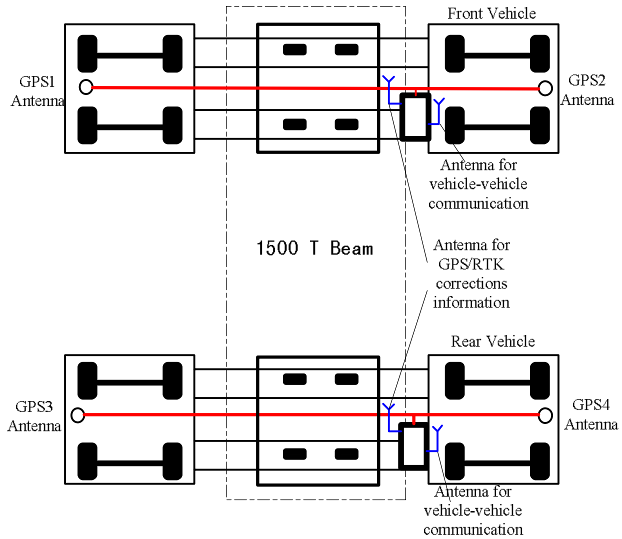

Figure 1. The schematic of the Twin Hoisting-Girder Transporters

system; Section IV introduces the practical application results; Conclusions are given at the end of the paper.

II. SYSTEM REQUIREMENTS AND THE VEHICLE KINEMATICS MODEL

Our research motivation is the coordinated control of a real large-scale transportation vehicles fleet, which was composed by two large-scale vehicles controlled by themselves.

Two transporters cooperate in handling large objects without rigid connecting component between them. In the collaborative work, the speed and orientation of the two vehicles must keep consistent. Master-slave mode was adopted for the coordinated control. The relative position deviation and orientation, speed errors of the two vehicles were accessed to control the rear one to follow the front one. We use symmetrical laid two RTK-GPS receivers to complete position and orientation measurement for a single vehicle, the in-vehicle speed sensors were used for speed measurement, wireless network communication devices were used for information exchange between two vehicles. The schematic of the transportation vehicles fleet is shown in Fig. 1.

The vehicle was driven in differential mode, the speed difference of two sides wheels decides the orientation of the vehicle, the average speed of them decides the vehicle's speed. Simplified schematic of one single vehicle in general global coordinate frame is shown in Fig. 2.

$\{X_b, Y_b\}$ denotes a body frame attached on the vehicle reference point P and $\{X, Y\}$ represent the global coordinate frame. l denotes the distance between wheel center and the reference point P, r denotes the radius of the wheel, ω_l and ω_r, respectively, denotes the angular rate of the left and right wheels, V denotes the velocity of the reference point P, and θ represents the orientation of the vehicle with respect to the X axis. We define the vector $[x, y]^T$ as the coordinate of

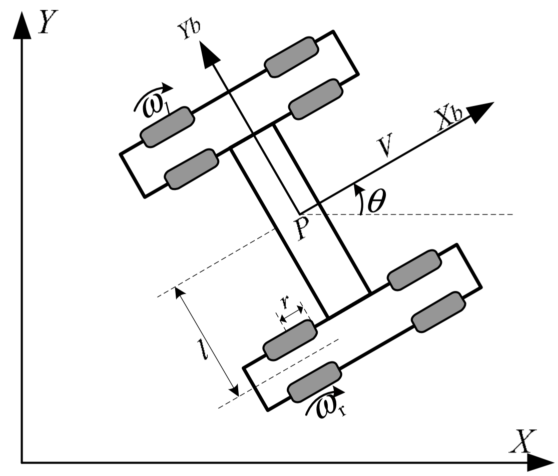

Figure 2. Simplified schematic of the vehicle

point P.

The posture kinematics model of the vehicle is as follows

$$\begin{cases} \dot{x} = v\cos(\theta) \\ \dot{y} = v\sin(\theta) \\ \dot{\theta} = \omega_z \end{cases}, \tag{1}$$

where

$$\begin{cases} v = \frac{1}{2} r(\omega_l + \omega_{\mathrm{r}}) \\ \omega_z = \frac{1}{2l} r(\omega_r - \omega_l) \end{cases}, \tag{2}$$

ω_z denotes the angular rate of the vehicle, ω_l and ω_{r} denote the measurements of two sides wheels' speed sensors. They can be described by

$$\begin{cases} \omega_l = \omega_{lt} + \varepsilon_{\mathrm{lr}} \\ \omega_{\mathrm{r}} = \omega_{rt} + \varepsilon_{\mathrm{rr}} \end{cases}, \tag{3}$$

ω_{lt} and ω_{rt} represent the true speed values, $\varepsilon_{\mathrm{lr}}$ and $\varepsilon_{\mathrm{rr}}$ denote speed sensors' measurement noises which are assumed to be zero mean Gaussian white noise with sampled variance of σ_{lr}^2 and σ_{rr}^2.

For the sake of convenience, the problem considered in this paper is to utilize the high-update speed sensors measurement and the lower update rate RTK-GPS measurement to estimate the posture $\{x, y, \theta\}$ and velocity v of the vehicle at an update rate that the speed sensor can provide. The measurement results were used for coordinated motion control of the twin transporters.

III. POSTURE AND VELOCITY KINEMATICS ESTIMATION SYSTEM

A. Kinematics estimation system

The whole architecture of the estimation scheme is shown in Fig. 3. The vehicle's posture and velocity are estimated by using the in-vehicle speed sensors and two RTK-GPS measurements based on the Extended Kalman Filter (EKF).

The estimation procedure is described as followed:

Step1: Initializing the whole estimation system.

Step2: High-update rate state prediction.

The speed sensors' measurement update rate is higher than that of the RTK-GPS receiver. At any time when there are no absolute GPS measurements, we estimate the posture and velocity by integrating the kinematics model (1), (2) using the high bandwidth in-vehicle speed sensors. This manner can provide a maximum update rate that the speed sensors can offer. But due to the integration inaccuracies, the velocity and orientation estimation errors grow linearly with time and the position error grows quadratically with time [7].

After this step finished, if there are still no new GPS measurements that can be used for observation prediction in step4, the procedure will directly jump to step5.

Step3: Low-update rate GPS measurement pre-processing.

Since RTK-GPS measurement contains several types of inherent noises, some of which do not satisfy the statistical assumptions commonly associated with the Kalman Filter, in this step, a GPS noise processing method was used to filter the raw measurement.

Step4: EKF-based state observation prediction.

When the low-update rate GPS measurement which was pre-processed in step3 are available, the posture and velocity are estimated by the Extended Kalman Filter (EKF) using the results of step2 and step3.

Step5: The posture and velocity estimation feedback to the coordinated motion control system.

Step6: Repeat from step2.

B. Low-update rate GPS measurement pre-processing

Two GPS antennas were symmetrically fixed at both sides of the vehicle to access the end points' coordinates. Then the coordinate of the vehicle center point P and the orientation of the vehicle can be calculated as follows

$$\begin{cases} x = \dfrac{x_l + \mathrm{x_r}}{2} \\ y = \dfrac{y_l + y_\mathrm{r}}{2} \\ \theta = \dfrac{\pi}{2} + \arctan(\dfrac{y_l - y_\mathrm{r}}{x_l - \mathrm{x_r}}) \end{cases} . \tag{4}$$

Since some of the noises in the RTK-GPS measurement do not satisfy the statistical assumptions commonly associated

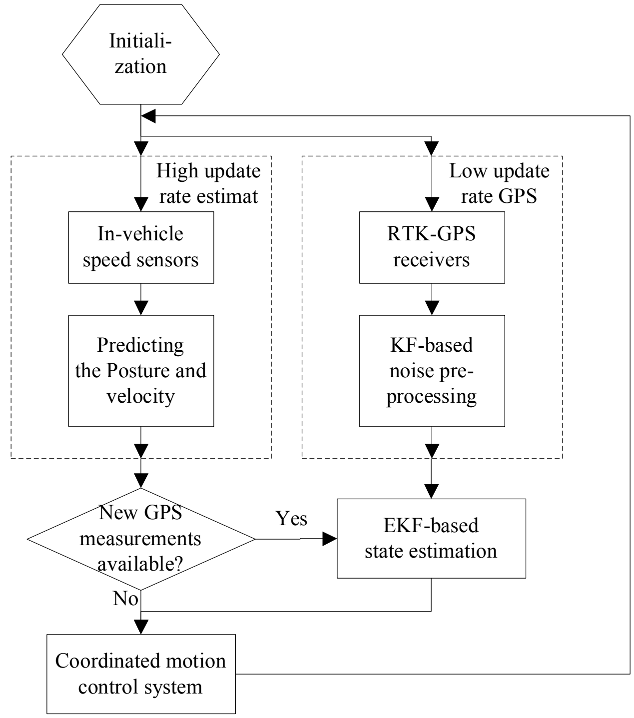

Figure 3. Architecture of the estimation scheme

with the Kalman filter, we need to pre-process the measurement to enhance the accuracy.

The measurement of the RTK-GPS can be described by

$$\begin{cases} x_m(k) = x(k) + \omega_\mathrm{x} + \varepsilon_\mathrm{xr} \\ y_m(k) = y(k) + \omega_\mathrm{y} + \varepsilon_\mathrm{yr} \end{cases}, \tag{5}$$

where $x_m(k)$ and $y_m(k)$ denote the RTK-GPS position measurements at time k, $x(k)$ and $y(k)$ denote the true position of the GPS antenna, ω_x and ω_y can be treated as constant which represents, respectively, bias in the RTK-GPS measurement, ε_xr and ε_yr denote the measurements noise which are assumed to be Gaussian white noise with a sampled variance of $\{\sigma_x^2, \sigma_y^2\}$.

We use Kalman filter to pre-process the measurements of the RTK-GPS. Setting the state vector $\mathbf{X} = [x, y, v_x, v_y, a_x, a_y]^T$, the observation vector $\mathbf{Z} = [L_x \ \ L_y]^T$ which is modified RTK-GPS measurement that are sent to the KF, and the discrete-time transition equation and observation equation sampled at time k can be described as

$$\begin{cases} \mathbf{X}_{k+1} = \mathbf{A}\mathbf{X}_k + \mathbf{W}_k \\ \mathbf{Z}_{k+1} = \mathbf{H}\mathbf{X}_k + \mathbf{V}_k \end{cases}, \tag{6}$$

where the transition matrix $\mathbf{A}$ is defined as

$$\mathbf{A}=\begin{bmatrix}1 & 0 & T & 0 & T^2/2 & 0\\ 0 & 1 & 0 & T & 0 & T^2/2\\ 0 & 0 & 1 & 0 & T & 0\\ 0 & 0 & 0 & 1 & 0 & T\\ 0 & 0 & 0 & 0 & 1 & 0\\ 0 & 0 & 0 & 0 & 0 & 1\end{bmatrix}.$$

The Kalman filter procedure is described as

$$\begin{cases}\mathbf{X}_{k+1/k}=\mathbf{A}\mathbf{X}_{k/k}\\ \mathbf{P}_{k+1/k}=\mathbf{A}\mathbf{P}_{k/k}\mathbf{A}^T+\mathbf{Q}\\ \mathbf{K}=\mathbf{P}_{k+1/k}(\mathbf{P}_{k+1/k}+\mathbf{R})^{-1}\\ \mathbf{X}_{k+1/k+1}=\mathbf{X}_{k+1/k}+\mathbf{K}(\mathbf{Z}_k-\mathbf{X}_{k+1/k})\\ \mathbf{P}_{k+1/k+1}=(\mathbf{I}-\mathbf{K})\mathbf{P}_{k+1/k}\end{cases}, \tag{7}$$

where $\mathbf{Q}$ and $\mathbf{R}$, respectively, is the covariance matrix of the discretized noise vector $\mathbf{W}_k$ and $\mathbf{V}_k$.

KF's strength is to deal with Gaussian white noises such as $\{\varepsilon_{\mathrm{xr}},\varepsilon_{\mathrm{yr}}\}$, since the variance changes frequently, in order to account for it, the correlation matrix $\mathbf{R}$ should be chosen intelligently. Under the dynamic driving scenarios, the KF designed for $\{\varepsilon_{\mathrm{xr}},\varepsilon_{\mathrm{yr}}\}$ is inefficient in dealing with the bias $\{\omega_{\mathrm{x}},\omega_{\mathrm{y}}\}$. Therefore, we need to deal with them separately.

Data received by user from GPS receivers is raw measurements and NMEA-GPG sentences which contain information such as position, GPS fix indicator, number of satellites in use, horizontal dilution of precision (HDOP) values, and time in seconds since last correction update, etc. We use this information and the data from speed sensors to deal with the two kinds of noise.

The rules that detect the biases $\{\omega_{\mathrm{x}},\omega_{\mathrm{y}}\}$ are by comparing the travel distance calculated from the current and the previous RTK-GPS measurements and that based on vehicle speed [8]. $[\Delta x_m(k),\Delta y_m(k)]^T$ is used to denote the position change from time $k-1$ to k calculated by RTK-GPS measurements, and $[\Delta x_c(k),\Delta y_c(k)]^T$ denotes the corresponding vehicle position change calculated using the vehicle speed and the time span T, then $[e_x(k),e_y(k)]^T=[\Delta x_m(k),\Delta y_m(k)]^T-[\Delta x_c(k),\Delta y_c(k)]^T$ denotes the calculated relative position error;

The rules are described as follows (Note: all of these rules based on the situation that the RTK-GPS is in the diff. status):

1) When the position error is small, it can be neglected:

If $\left\|\begin{bmatrix}e_x(k)\\ e_y(k)\end{bmatrix}\right\|_2<\varepsilon_{small}$, then $\begin{bmatrix}x_m'(k)\\ y_m'(k)\end{bmatrix}=\begin{bmatrix}x_{\mathrm{m}}(k)\\ y_m(k)\end{bmatrix}$;

2) The position error can still be accepted:

If $\varepsilon_{small}<\left\|\begin{bmatrix}e_x(k)\\ e_y(k)\end{bmatrix}\right\|_2<\varepsilon_{large}$, then $\begin{bmatrix}x_m'(k)\\ y_m'(k)\end{bmatrix}=\begin{bmatrix}x_{\mathrm{m}}(k)\\ y_m(k)\end{bmatrix}-\alpha\begin{bmatrix}e_x(k)\\ e_y(k)\end{bmatrix}$, $0\le\alpha\le 1$;

3) Large error:

If $\varepsilon_{large}<\left\|\begin{bmatrix}e_x(k)\\ e_y(k)\end{bmatrix}\right\|_2$, then the RTK-GPS measurement is discarded and the KF continues without updating GPS measurement.

Here $[x_m'(k),y_m'(k)]^T$ are the modified RTK-GPS measure-ements that are sent to the KF. Furthermore, ε_{small} and ε_{large} are the position error bounds that are functions of vehicle speed and RTK-GPS update frequency.

The determination of $\mathbf{R}$ is related with the HDOP (hdop), GPS fix indicator (fix_status), number of satellites (sat_num) and time since last correction update (time_error). It can be described as nonlinear functions:

$$\mathbf{R}=\mathbf{F}(hdop, fix\_status, sat\_num, time\_error). \tag{8}$$

The rules are described as follows:

1) When the GPS fix indicator data is "2", which means that the RTK-GPS measurement is in differential status, if $time\_error<10, H_i\le hdop<H_{i+1}$ and $N_j\le sat\_num<N_{j+1}$, then $R_x=VarX_{ij}$, $R_y=VarY_{ij}$;

2) If (fix_status = normal or fix_status = invalid) or (fix_status = diff. and $10\le time\_error$) then $R_x=R_y=R_{\max}$.

Here $\mathbf{R}=diag(R_x,R_y)$, with R_x and R_y corresponding to the variance of RTK-GPS measurement of x and y. $R_{\max}$ is a very large number so that the RTK-GPS measurement has little effect on the KF.

C. Discrete kinematics model

The discrete-time vehicle state transition equation is [9]

$$\mathbf{x}_{k+1}=\mathbf{f}(\mathbf{x}_k,k)+\mathbf{w}_k, \tag{9}$$

where

$$\mathbf{f}(\mathbf{x}_k,k)=\begin{bmatrix}x_k+\frac{1}{2}r\Delta t(\omega_{\mathrm{l}k}+\omega_{\mathrm{r}k})\cdot\cos(\theta_k)\\ y_k+\frac{1}{2}r\Delta t(\omega_{\mathrm{l}k}+\omega_{\mathrm{r}k})\cdot\sin(\theta_k)\\ \theta_k+\frac{1}{2l}\Delta t(\omega_{\mathrm{l}k}-\omega_{\mathrm{r}k})\\ \omega_{\mathrm{l}k}\\ \omega_{\mathrm{r}k}\end{bmatrix}. \tag{10}$$

The state vector is $\mathbf{x}_k = [x_k, y_k, \theta_k, \omega_{1k}, \omega_{rk}]^T$, and the process noise vector is $\mathbf{w}_k = [0, 0, 0, \Delta t\varepsilon_{lr}, \Delta t\varepsilon_{rr}]^T$. Δt denotes the sample time of the discrete system.

The observation vector is denoted as $\mathbf{z}_k = [z_{xk}, z_{yk}, z_{\theta k}, z_{1k}, z_{rk}]^T$, and the observation equations sampled at time can be described as

$$\mathbf{z}_k = \mathbf{h}(\mathbf{x}_k) + \mathbf{v}_k, \tag{11}$$

where $\mathbf{h}(\mathbf{x}_k) = [x_k, y_k, \theta_k, \omega_{1k}, \omega_{rk}]^T$, and observation noise vector is $\mathbf{v}_k = [v_{xk}, v_{yk}, v_{\theta k}, v_{1k}, v_{rk}]^T$.

D. High-update rate state prediction

At the time k when absolute GPS measurement is not available, the posture $[x_k, y_k, \theta_k]^T$ and velocities $[\omega_{1k}, \omega_{rk}]^T$ are estimated as followed

$$\hat{\mathbf{x}}_{k+1}^- = \mathbf{f}(\hat{\mathbf{x}}_k, k). \tag{12}$$

The error covariance between the true state and the estimated state $\hat{\mathbf{x}}_{k+1}^-$ is given by

$$\mathbf{P}_{k+1}^- = \mathbf{\Phi}\mathbf{P}_k\mathbf{\Phi}^T + \mathbf{Q}_K. \tag{13}$$

$\mathbf{\Phi}$ denotes the Jacobian of $\mathbf{f}(\mathbf{x}_k)$ at time k, and $\mathbf{Q}_K$ is the covariance matrix of the discretized noise vector $\mathbf{w}_k$.

This process is repeated at the high update rate that the speed sensors can provide. But if at the time k, the EKF-based estimation which was described in Part E is available, the $\hat{\mathbf{x}}_k$ and $\mathbf{P}_k$ will choose the results of it, otherwise the last results of this process will be chosen.

E. EKF-based state observation prediction

When the RTK-GPS measurement is available, the $\mathbf{z}_k$ in (12) now can be used.

Based on the predicated state $\hat{\mathbf{x}}_k^-$, we have the predicted observation

$$\hat{\mathbf{z}}_k = \mathbf{h}(\hat{\mathbf{x}}_k^-). \tag{14}$$

We define the prediction observation error as

$$\boldsymbol{\alpha}_k = \mathbf{z}_k - \hat{\mathbf{z}}_k, \tag{15}$$

with the covariance

$$\mathbf{S}_k = \mathbf{H}\mathbf{P}_k^-\mathbf{H}^T + \mathbf{R}_k. \tag{16}$$

$\mathbf{H}$ denotes the Jacobian of $\mathbf{h}(\cdot)$ where $\mathbf{R}_k$ is the covariance matrix of the measurement noise.

Then we define the Kalman gain as

$$\mathbf{K}_k = \mathbf{P}_k^-\mathbf{H}^T\mathbf{S}_k^{-1}. \tag{17}$$

The state estimate and covariance update equations of the EKF are as followed

$$\begin{cases} \hat{\mathbf{x}}_k^+ = \hat{\mathbf{x}}_k^- + \mathbf{K}_k \cdot \boldsymbol{\alpha}_k \\ \mathbf{P}_k^+ = (\mathbf{I} - \mathbf{K}_k\mathbf{H})\mathbf{P}_k^- \end{cases}. \tag{18}$$

Based on this process, we can access more accurate posture and velocity, and at the same time, the integration errors which accumulate at the step2 are reset. At the next sample time $k+1$, the estimate results will be chosen for high-update rate state prediction.

IV. PRACTICAL APPLICATION

A. Application setup

Two sets of this system were fitted on the two Hoisting-Girder Transporters respectively. The working status is shown in Fig. 4.

As shown in Fig. 5, two NovAtel FlexPak-G2L-L1L2 dual-frequency RTK-GPS receivers which have horizontal position accuracy of ±1cm RMS are laid on both sides of the transporter.

An embedded Touching-PC (TPC) with WinCE operating system hosts the twin transporter coordinated motion control software. The software is written using EVC4.0. The TPC also has a CAN-BUS interface port enabling it to communicate with the speed sensors.

Figure 4. Working status of twin hoisting-girder transporters

Figure 5. User RTK-GPS antenna and receiver

The user GPS receivers are programmed to provide measurements at an update rate of 5Hz and the speed sensors are sampled at a higher update rate at 20Hz.

B. *Application results*

Stationary measurement was done in outdoor obstacle free environment over half a hour period to test the KF-based GPS data noise filter method. The base station data was taken after twenty minutes warming up. The data was calculated using the online algorithms mentioned on Section III, and the results were saved and plotted using software Excel as shown in Fig. 6.

It shows that the noise preprocess-based EK leads to good estimation accuracy for a single point RTK-GPS measurement, which is useful for enhancing the accuracy of the vehicle' posture and velocity estimation.

Fig.7 shows the actual application results. The top figure showed the orientation deviation between two transporters and the bottom figure showed the relative distance of the two vehicles. Clearly, the proposed method allows a high update rate and accurate posture, velocity estimation for the coordinated control. The whole system has been successfully used in a cross-sea bridge construction project.

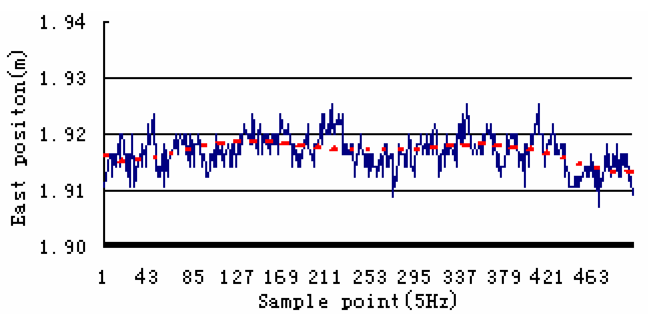

Figure 6. Stationary measurement results

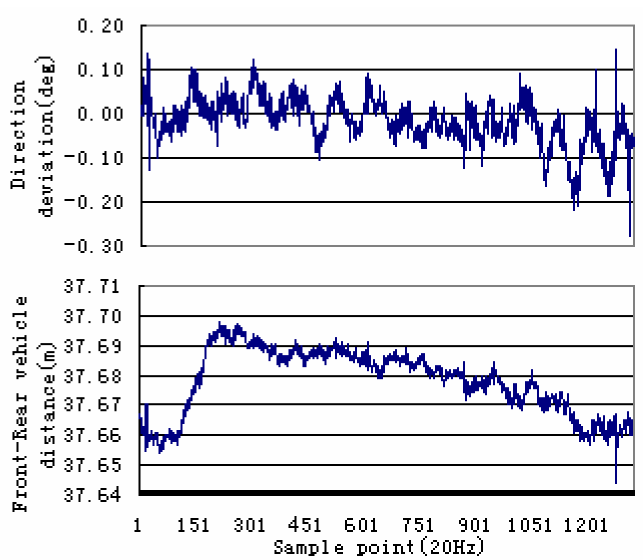

Figure 7. The application results measurement

V. CONCLUSIONS

This paper presents the development of a high-update rate and accurate vehicle posture and velocity estimation system using the RTK-GPS units and relatively simple in-vehicle speed sensors. KF-based RTK-GPS measurement estimation method divided the noise into two parts, one of which can be seen as a constant that will be discarded and another part can be easily removed by KF. The method facilitates fast initialization and fast recovery without sacrificing estimation accuracy and integrity.

The combination of the low-update rate RTK-GPS measurement and high-update rate in-vehicle speed sensor measurement enhances the update rate of the vehicle's posture and velocity estimation to the high-update rate that the speed sensors can afford. With these high-update rate estimates, the fleet coordinated control laws can be applied more effectively and reliably.

This method can be applied to the accurate location of different vehicle fleets such as people transportation or goods transportation where the position information must known accurately and continuously (traveler information systems, security systems, surveillance system, etc.) .

ACKNOWLEDGMENT

The authors would like to thank the anonymous reviewers for their insightful comments.

REFERENCES

[1] H. Wei-Chung, F. Li-Chen, and H. Shin-Shinh, "Vision based obstacle warning system for on-road driving," in Proc. IEEE/RSJ Int. Conf. Intell. Robots Syst., Las Vegas, NV, vol. 4, pp. 3668-3673, Oct. 27–31, 2003.

[2] L. Moon-Silk and K. Yong-Hoon, "An efficient multitarget tracking algorithm for car applications," IEEE Trans. and. Electron., vol. 50, no. 2, pp.397-399, Apr. 2003.

[3] D. M. Bevly, "GPS: A low cost velocity sensor for correcting inertial sensor errors on ground vehicles," J. Dyn. Syst., Meas., Contr., vol. 126, no. 2, pp. 255-264, Jun. 2004.

[4] E. Abbott and D. Powell, "Land-vehicle navigation using GPS," Proceedings of IEEE, vol. 87, no. 1, pp: 145-162, Jan, 1999.

[5] R. Da, G. Dedes, and K. Shubert, "Design and analysis of a high-accuracy airborne GPS/INS system," in Proc. 9th Int. Techn. Meeting Satellite Div. Inst. Navigation(GPS-96), pp. 955-964, 1996.

[6] D. M. Bevly, R. Sheridan and J. C. Gerdes, "Integrating INS sensors with GPS velocity measurements for continuous estimation of vehicle sideslip and tire cornering stiffness," in IEEE Proceeding of the American Control Conference, vol. 4, pp: 25-30, June, 2000.

[7] S. Sukkarieh, E. M. Nebot and H. F. Durrant Whyte, "A high integrity IMU/GPS navigation loop for autonomous land vehicle application," IEEE Transactions on Robotics and Automation, vol. 15, no. 3, pp. 572-578, June, 1999.

[8] J. H. Huang and H. S. Tan, "A low-order DGPS-Based vehicle positioning system under urban environment," IEEE Transactions on mechatronics, vol. 11, no. 5, pp. 567-575, October, 2006.

[9] C. B. Low and D. W. Wang, "Integrated Estimation for wheeled mobile robot posture, velocities, and wheel skidding perturbations," IEEE Int. Conf. Robotics and Automation, Roma, Italy, pp. 2355-2360, April 2007.